

## High temperature oxidation of Al<sub>2</sub>O<sub>3</sub>-based composites with Ni particle dispersion

Makoto Nanko\*, Nguyen Dang Thuy, Koji Matsumaru and Kozo Ishizaki

Department of Mechanical Engineering, Nagaoka University of Technology, Nagaoka, Niigata 940-2188, Japan

The oxidation behavior of Al<sub>2</sub>O<sub>3</sub>-based composites with a 5 vol% Ni particle dispersion was investigated at high temperatures in air. The oxidized layer consisted of Al<sub>2</sub>O<sub>3</sub> and NiAl<sub>2</sub>O<sub>4</sub>. The growth of the oxidized layer followed a parabolic manner, which means that mass transport in the oxidized layer was the rate-controlling process. The value of the parabolic rate constant at 1300°C was  $1.8 \times 10^{-14} \text{ m}^2 \text{ s}^{-1}$  which is higher than those of SiC-dispersed Al<sub>2</sub>O<sub>3</sub> composites and Al<sub>2</sub>O<sub>3</sub>-former alloys.

**Key words:** high temperature oxidation, nickel, alumina, NiAl<sub>2</sub>O<sub>4</sub>, composites.

### Introduction

To increase conversion efficiency of thermal cycles such as gas turbine engines, new high temperature materials are required. Functionally graded materials (FGMs) and nano-composites consisting of oxide ceramics and metals have received attention as the next generation of high temperature materials. They are classified as metal-dispersed oxide composites. Their mechanical and physical properties have been studied as well as their production processes [1, 2]. However the high temperature oxidation/corrosion of metal-dispersed oxide composites has not been investigated in any details. Only the high temperature oxidation of thermal barrier FGM coatings has been reported [3]. There are also a few reports on the oxidation behavior of oxide ceramics with non-oxide ceramic dispersion such as SiC or TiN [4-8].

Since at high temperatures oxygen can pass through oxide matrix, a metallic dispersion will oxidize in the matrix. The metallic dispersion expands due to oxidation and stresses the matrix. The matrix is cracked when the stress generated by the oxidation of the metal dispersion reaches the fracture strength. Finally, the composite is fractured. Thus, to design FGMs and nano-composites for high temperature applications, high temperature oxidation/corrosion is very important.

Nanko *et al.* [9, 10] reported on the high temperature oxidation of partially-stabilized zirconia (PSZ) composites with Ni particle dispersions. Due to the oxidation of the Ni dispersion, the PSZ matrix was cracked in the surface region. The cracked region grew proportionally with oxidation time. Based on a kinetic analysis of oxidation, they concluded that the fracture

of the matrix was due to the oxygen permeation of the PSZ and the growth rate of the cracked zone depended on the partial hole conductivity of the PSZ, which dominated the oxygen permeation.

Taking account of their results of PSZ composites, an oxide with high oxygen permeability is not suitable as a matrix. Alumina, which is one of the most popular ceramics, has excellent mechanical properties and low diffusivity of ions at high temperatures. In this paper, high temperature oxidation of Al<sub>2</sub>O<sub>3</sub>-based composites with an Ni particle dispersion is discussed.

### Experimental

Commercial  $\alpha$ -alumina powder (Sumitomo Chemical Co., AA-04, with a particle size 0.5  $\mu\text{m}$ , and purity 99.99%) with 5 vol % of Ni powder (purity 99%, 10  $\mu\text{m}$ ) were mixed in ethyl alcohol for 30 minutes in a mortar. After drying, the powder mixture was consolidated using a pulsed current pressure-sintering technique at 1350°C in die temperature under 40 MPa die pressure for a 30 minutes holding time in vacuum. The sintered samples attained a density of at least 99% of theoretical value. The surface of the samples was ground using #1500 SiC-abrasive papers. The sample was put on top of alumina balls in an alumina crucible and oxidized at 1300 and 1350°C in air. The heating rate in the oxidation experiments was 400 K/h. The oxidized samples were evaluated using X-ray diffraction (XRD) to identify the oxidation products and scanning electron microscopy (SEM) to observe the microstructure.

### Results and Discussion

Figure 1 shows the XRD pattern of the surface of a sample after oxidation at 1300°C for 5 days. There are peaks of  $\alpha$ -Al<sub>2</sub>O<sub>3</sub>, NiAl<sub>2</sub>O<sub>4</sub> in the XRD pattern. Peaks of NiO cannot be identified clearly. This fact means

\*Corresponding author:  
Tel : +81-258-47-9709  
Fax: +81-258-47-9770  
E-mail: nanko@mech.nagaokaut.ac.jp

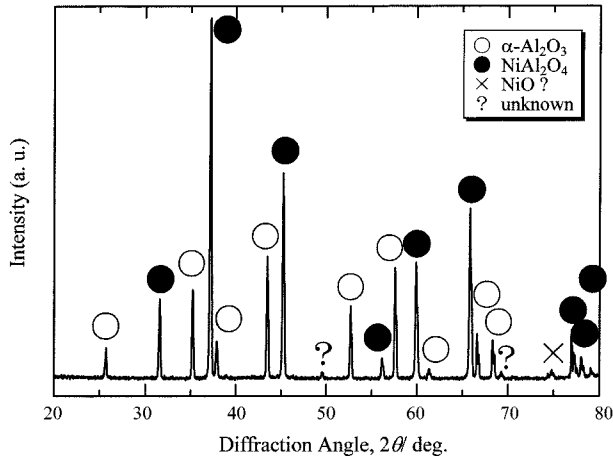
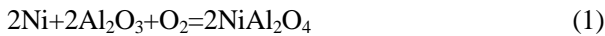


**Fig. 1.** XRD pattern of Al<sub>2</sub>O<sub>3</sub> composite with Ni dispersion after oxidized at 1300°C for 5 days.

that the oxidation reaction of Ni particles in the Al<sub>2</sub>O<sub>3</sub> matrix follows the equilibrium phase relation as follows:



Based on the ternary phase diagram of Ni-Al-O [11], NiO does not coexist with Al<sub>2</sub>O<sub>3</sub> and NiAl<sub>2</sub>O<sub>4</sub>.

Figure 2 shows an SEM image of the sample surface after oxidation at 1300°C for 2 days. The surface of the oxidized sample consists of flat area, represents the initial surface, and well-faceted nodules. With increasing oxidation time or temperature, the well-faceted nodules grew and covered the surface. Figure 3 shows an SEM photograph of a cross-sectional view of the sample oxidized at 1300°C for 5 days. As shown in Fig. 3, there are no Ni particles in the region from the surface to a depth of 95 μm. The region in which Ni particles have oxidized completely is defined as the oxidized layer. The metallic Ni dispersion has been oxidized completely in this region. The Al<sub>2</sub>O<sub>3</sub> composite is not fractured by the oxidation of the Ni particles at all. There is a surface layer that has a

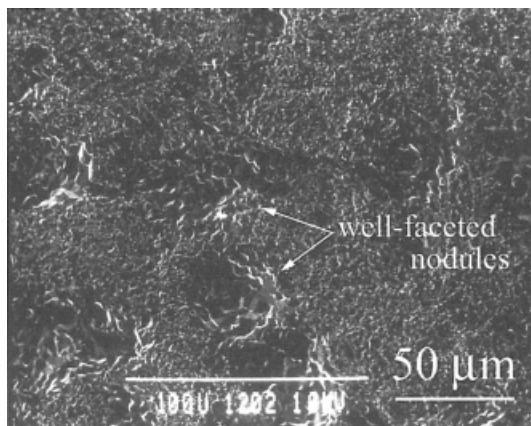


**Fig. 2.** SEM image of sample surface after oxidation at 1300°C for 2 days.

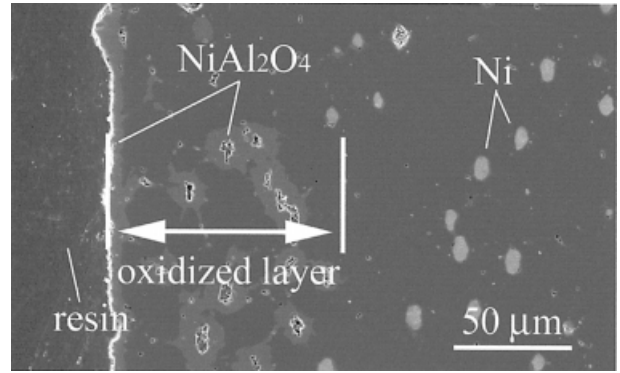


**Fig. 3.** Cross-sectional SEM image of sample after oxidation at 1300°C for 5 days.

different color with the Al<sub>2</sub>O<sub>3</sub> matrix and is similar to the oxidized dispersion in the oxidized region. The top layer and the oxidized dispersion can be identified as NiAl<sub>2</sub>O<sub>4</sub> based on the results of XRD. NiAl<sub>2</sub>O<sub>4</sub> grains in the oxidized layer are irregular in shape, compared with Ni particles. They have extrusions into the Al<sub>2</sub>O<sub>3</sub> matrix. Voids are also observed in the NiAl<sub>2</sub>O<sub>4</sub> dispersion located in the oxidized zone. Between the oxidized layer and the non-oxidized region, there is an intermediate region which consists of partially-oxidized Ni particles.

From the surface, there are 3 regions with (1) completely oxidized Ni particles, (2) partially oxidized particles, and (3) Ni particles where an oxide layer is not observed. In this paper, region (1) is defined as an oxidized layer.

Figure 4 shows the depth of the oxidized layer, *x*, as a function of holding time, *t*, for the high temperature oxidation of a 5 vol% Ni-dispersed Al<sub>2</sub>O<sub>3</sub> composite. Growth of the oxidized region follows a parabolic manner:

$$x^2 = k_p t \quad (2)$$

where *k<sub>p</sub>* is the parabolic rate constant. Since the oxidized region is dense as shown in Fig. 3, mass

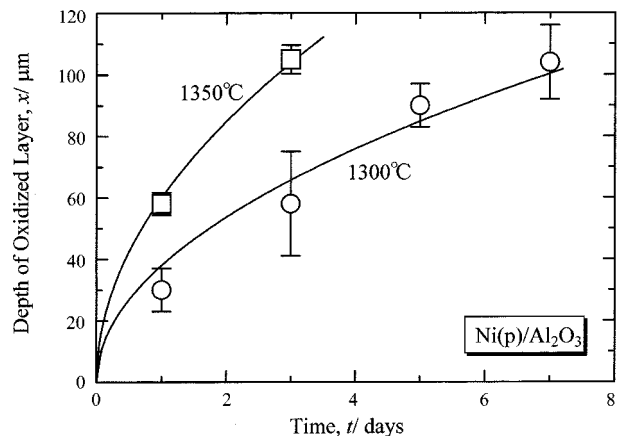


**Fig. 4.** Depth of oxidized layer, *x*, as a function of time, *t*, on high temperature oxidation of 5 vol% Ni-dispersed Al<sub>2</sub>O<sub>3</sub>.

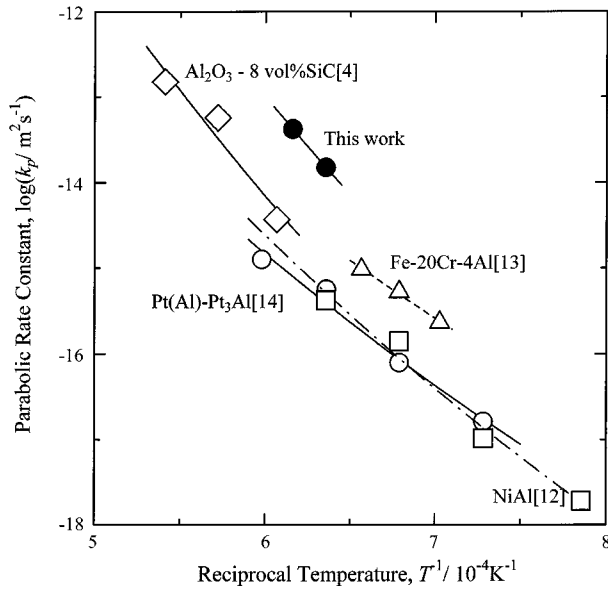


Fig. 5. Comparison of parabolic rate constant with different materials.

transport through the oxidized layer is the predominant process for the growth of the oxidized layer. Figure 5 shows the parabolic rate constant as a function of reciprocal temperature. The values of  $k_p$  for some high temperature materials are given in Fig. 5. The oxidation resistance of the  $\text{Al}_2\text{O}_3$ -based composites with 5 vol% Ni particles is less than those of SiC-dispersed  $\text{Al}_2\text{O}_3$  composites [4] and  $\text{Al}_2\text{O}_3$ -forming alloys [12-14]. The temperature dependence of  $k_p$  on the growth of the oxidized layer of Ni-dispersed  $\text{Al}_2\text{O}_3$  is similar to that of other materials.

As shown in Fig. 2, heterogamous  $\text{NiAl}_2\text{O}_4$  forms on the initial surface. The initial surface was also observed on the surface after oxidation. This morphology means that the faceted surface, consisting of  $\text{NiAl}_2\text{O}_4$  developed by the outward diffusion of cations along grain boundaries. Figure 6 illustrates the mechanism of the growth of this oxidized layer. In the case where cations were not supplied from the inside, the surface should be flat after oxidation. Such surface morphology can be

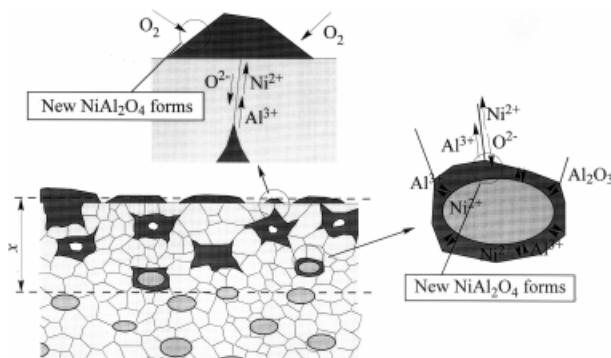


Fig. 6. Schematic illustration of a speculation of the mechanism of high temperature oxidation of Ni-dispersed  $\text{Al}_2\text{O}_3$  composite.

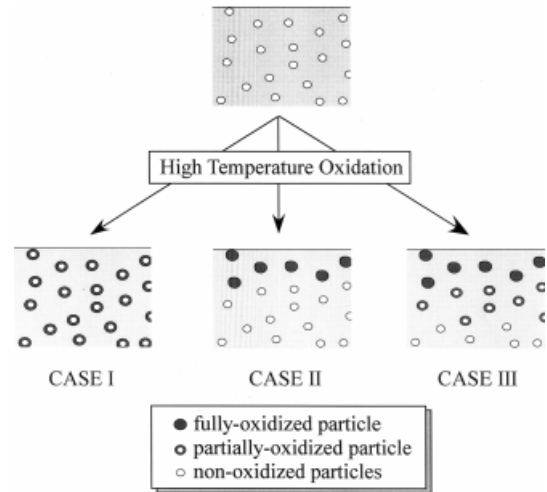


Fig. 7. Schematic illustration of oxidation modes of oxide ceramics composites [4].

observed in the high temperature oxidation of  $\text{Al}_2\text{O}_3$ -forming alloys that develop an  $\text{Al}_2\text{O}_3$  scale with a large contribution from the outward diffusion of Al along grain boundaries [13, 15-17]. The voids in the  $\text{NiAl}_2\text{O}_4$  in the inside of the oxidized layer are also developed due to the outward diffusion of cations. Because the volume expansion of the dispersion by oxidation is compensated due to the outward diffusion of cations, fracture of the oxidized zone does not occur.

Luthra and Park [4] reported on the oxidation behavior of SiC-dispersed oxide ceramic composites at temperatures ranging from 1375 to 1575°C. As shown in Fig. 7, they described three possible situations in their oxidation behavior, which depend on the relative diffusion rates or permeabilities of oxygen through the matrix oxide and the reaction products:

CASE I; oxygen diffusion rate through the matrix oxide is much faster than the oxide production rate,

CASE II; oxygen diffusion rate through the oxidation product is comparable to or faster than that through the matrix oxide, and

CASE III; an intermediate situation between case 1 and 2.

The oxidation behavior of Ni particle-dispersed  $\text{Al}_2\text{O}_3$  composites in this study corresponds to CASE III, as observed in Fig. 3. As shown in Fig. 3, the shape of  $\text{NiAl}_2\text{O}_4$  grains is irregular. Extrusions of  $\text{NiAl}_2\text{O}_4$  into the  $\text{Al}_2\text{O}_3$  matrix are observed in the oxidized layer. The extrusions are formed due to the rate-controlling supply of oxygen to the Ni grains, which occurs in CASE II or CASE III. To decrease the distance of diffusion of oxygen,  $\text{NiAl}_2\text{O}_4$  grows along the grain boundaries of the  $\text{Al}_2\text{O}_3$  matrix, as shown in Fig. 6.

Based on the discussion above, the growth of the oxidized layer is predominately a mass transport process

along the grain boundaries in the oxidized layer. However, the dominant diffusion species in the polycrystalline  $\text{Al}_2\text{O}_3$  is not obvious in the research on high temperature oxidation of  $\text{Al}_2\text{O}_3$ -forming alloys [16-23]. Chida *et al.* [24] reported that the contribution of grain boundary diffusion of cations to growth of  $\text{Al}_2\text{O}_3$  scale was from 30 to 50% during high temperature oxidation of NiAl. The oxidation rate of Ni dispersed- $\text{Al}_2\text{O}_3$  is much faster than that of the  $\text{Al}_2\text{O}_3$  forming alloys such as NiAl. Grain boundary diffusion through the oxidized layer consisting of  $\text{Al}_2\text{O}_3$  and  $\text{NiAl}_2\text{O}_4$  may be much faster than in the pure  $\text{Al}_2\text{O}_3$  scale due to the influences of doping of NiO or by the formation of an  $\text{NiAl}_2\text{O}_4$  grain boundary phase. In this research, the predominant process for the growth rate of the oxidized layer remains unclarified as yet.

### Conclusions

The oxidation behavior of  $\text{Al}_2\text{O}_3$ -based composites with a 5 vol% Ni particle dispersion was investigated at high temperatures in air. The oxidized layer consisted of  $\text{Al}_2\text{O}_3$  and  $\text{NiAl}_2\text{O}_4$ . The growth of the oxidized layer followed a parabolic manner, which means that mass transport in the oxidized layer was the rate-controlling process. The growth of the oxidized layer was dominated by mass transport along the grain boundaries in the oxidized layer. The formation of  $\text{NiAl}_2\text{O}_4$  on the initial surface occurs by the outward diffusion of cations along the grain boundary of the oxidized layer. Since outward diffusion of cations can decrease the internal stress by the formation of oxide, the oxidized layer is not cracked, in contrast with the oxidation of zirconia ceramics with Ni particle dispersions.

### References

1. S. Sampath, H. Herman, N. Shimoda and T. Saito, MRS Bull. 20[1] (1995) 27-31.
2. T. Sekino, Y. Choa, A. Nakahira and K. Niihira, *Materia*, 38[5] (1999) 425-428.
3. M. Yoshiba, J. Gas Turbine Soc. Jpn. 25[3] (1998), 18-25.
4. K.L. Luthra and H.D. Park, J. Amer. Ceram. Soc. 73[4] (1990) 1014-1023.
5. M.P. Borom, M.K. Burn and L.E. Szala, *Adv. Ceram. Mater.* 3[5] (1988) 491-497.
6. M.I. Osendi, J. Mater. Sci. 25[8] (1990) 3561-3565.
7. M. Backhaus-Ricout, J. Amer. Ceram. Soc. 74[8] (1991) 1793-1803.
8. C.Y. Tsai and C.C. Lin, J. Amer. Ceram. Soc. 81[12] (1998) 3150-3156.
9. M. Nanko, M. Yoshimura and T. Maruyama, *Abst. 13<sup>th</sup> Fall Meeting Ceram. Soc. Jpn.* (2000) p.229.
10. M. Nanko, M. Yoshimura and T. Maruyama, *Abst. 128<sup>th</sup> Spring Meeting Jpn. Inst. Metals* (2001) p.188.
11. A.E. McHale and R.S. Roth, *Phase Equilibria Diagrams*, Vol. 12, (The American Ceramic Society, 1996) pp. 11-13.
12. F.S. Pettit, *Trans Metal. Soc. AIME* 239[9] (1967) 1296-1305.
13. T. Amano, S. Yajima and Y. Saito, J. Jpn. Inst. Met. 41[10] (1977) 1074-1082.
14. M. Nanko, M. Ozawa and T. Maruyama, *J. Electrochem. Soc.* 147[1] (2000) 283-288.
15. J.S. Sheasby and D.B. Jory, *Oxi. Met.* 12[6] (1978) 527-539.
16. P. Fofstad, "High Temperature Corrosion" (Elsevier, 1988) pp. 408-410.
17. J. Jedlinski and S. Mrowec, *Mater. Sci. Eng.* 87[1] (1972) 281-287.
18. F.A. Colightly, F.H. Stott and G.C. Wood, *J. Electrochem. Soc.* 126[6] (1979) 1035-1042.
19. F.H. Stott, G.C. Wood and J. Stringer, *Oxid. Met.* 44[1/2] (1995) 113-145.
20. R. Prescott and M.J. Graham, *Oxid. Met.* 38[3/4] (1992) 233-254.
21. E.W.A. Young, H.E. Bishop and J.H.W. De Wit, *Surf. Interface Anal.* 9[1-6] (1986) 163-168.
22. W.J. Quadackers, H. Holzberecher, H.G. Brief and H. Beske, *Oxid. Met.* 39[1/2] (1989) 67-88.
23. A. Pint, J.R. Martin and L.W. Hobbs, *Oxid. Met.* 39[3/4] (1993) 167-195.
24. T. Chida, M. Nanko, K. Kawamura and T. Maruyama, *129<sup>th</sup> Fall Meeting Jpn. Inst. Metals* (2001) p.316.